

# Vibrational Circular Dichroism of Polypeptides. 9. A Study of Chain Length Dependence for $3_{10}$ -Helix Formation in Solution

S. C. Yasui,<sup>†</sup> T. A. Keiderling,<sup>\*†</sup> F. Formaggio,<sup>‡</sup> G. M. Bonora,<sup>‡</sup> and C. Toniolo<sup>\*†</sup>

Contribution from the Department of Chemistry, University of Illinois at Chicago, Chicago, Illinois 60680, and Department of Organic Chemistry, Biopolymer Research Center, CNR, University of Padova, 35131 Padova, Italy. Received January 30, 1986

**Abstract:** Vibrational circular dichroism (VCD) and IR absorption spectra of the protected Z-(Aib)<sub>n</sub>-L-Leu-(Aib)<sub>2</sub>-OMe ( $n = 0-5$ ) oligopeptide series in CDCl<sub>3</sub> have been measured in the amide A, amide I, and amide II regions. For all three regions, the magnitudes of  $\Delta\epsilon/\epsilon$  measured indicate full development of the right-handed  $3_{10}$ -helical VCD at  $n = 3$ . The data also indicate that VCD of a similar band shape appears with reduced magnitude as early as  $n = 1$ , which is equivalent to two consecutive type III  $\beta$ -turns. The determination of this type of ordered conformation was confirmed by means of <sup>1</sup>H nuclear magnetic resonance. Such a solution conformation is consistent with the X-ray diffraction crystal structure of the two highest oligomers.

Vibrational circular dichroism (VCD) has been demonstrated to be a viable technique for differentiation of secondary structures of polypeptides.<sup>1-11</sup> Lal and Nafie<sup>2</sup> and Sen and Keiderling<sup>3</sup> have shown that the right-handed  $\alpha$ -helical conformation of a poly-(L-amino acid) gives rise to a positive couplet<sup>12</sup> (positive to lower energy) for the amide I band, a couplet of opposite sense for the amide A band, and a negative monosignate amide II band. The VCD sign pattern depends upon the helical sense and not on the chirality of the  $\alpha$ -carbon.<sup>2,3</sup> For a deuterated right-handed  $\alpha$ -helix, the amide I VCD is changed into a three-peak (-,+,-) pattern.<sup>3,6,11</sup> The amide I VCD of two, reported random coil polypeptides has been shown to be a negative couplet with a slight negative bias; however, there is no change in their VCD line shape upon deuteration.<sup>6</sup> The parallel and perpendicular amide I bands of an antiparallel  $\beta$ -sheet (at 1690 and 1630 cm<sup>-1</sup>, respectively) appears to give weak monosignate negative VCD peaks.<sup>11</sup>

The ability of Aib ( $\alpha$ -aminoisobutyric acid or  $\alpha,\alpha$ -dimethylglycine) to promote helical folding in peptides, due to the steric interactions of the *gem*-methyl groups attached to the  $\alpha$ -carbon atom, is well documented.<sup>13-17</sup> These studies indicate that linear oligopeptides containing Aib residues have mainly either  $\alpha$ -helical ( $\phi = \pm 55^\circ$ ,  $\psi = \pm 45^\circ$ ) or  $3_{10}$ -helical ( $\phi = +60^\circ$ ,  $\psi = \pm 30^\circ$ ) structures. Recently, the Padova laboratory has reported a reliable oligopeptide molecular model for the  $3_{10}$ -helix in which all or most of the residues are Aib.<sup>18-28</sup> VCD spectra in the 3600-1250-cm<sup>-1</sup> region of two monodispersed protected octapeptides, Z-(Aib)<sub>3</sub>-L-Val-Gly-L-Leu-(Aib)<sub>2</sub>-OMe (A<sub>3</sub>VGLA<sub>2</sub>) and Z-(Aib)<sub>5</sub>-L-Leu-(Aib)<sub>2</sub>-OMe (A<sub>5</sub>LA<sub>2</sub>), where Z is benzyloxycarbonyl and OMe is methoxy, in CDCl<sub>3</sub> have previously been reported by us.<sup>7</sup> The spectra are qualitatively similar to those of a right-handed  $\alpha$ -helix, but the magnitude of the amide I VCD couplet is much smaller than that of the amide II, and the asymmetry of both the amide I and A couplets is qualitatively reduced as compared to that found for the  $\alpha$ -helix. In order to obtain more information and extend the application of VCD to problems involving the  $3_{10}$ -helical and  $\beta$ -turn conformations, in this paper we report the IR absorption, VCD, and <sup>1</sup>H NMR spectral characterization of the set of protected oligopeptides Z-(Aib)<sub>n</sub>-L-Leu-(Aib)<sub>2</sub>-OMe (A<sub>n</sub>LA<sub>2</sub>) where  $n = 0-5$  in CDCl<sub>3</sub> solution. A preliminary communication of part of the results described herein has been reported.<sup>9</sup> Structural analyses of A<sub>4</sub>LA<sub>2</sub> and A<sub>5</sub>LA<sub>2</sub> by X-ray diffraction have established the tendency of these hepta- and octapeptides to adopt a right-handed  $3_{10}$ -helical conformation in the crystalline state.<sup>29</sup> Our results will demonstrate that this tendency also is evident in the solution phase.

## Experimental Section

**Synthesis of Peptides.** The details of the synthesis and physicochemical and analytical properties of Z-(Aib)<sub>n</sub>-L-Leu-(Aib)<sub>2</sub>-OMe ( $n = 5$ )

have already been described.<sup>7</sup> Similar data on the lower homologues ( $n = 0-4$ ) will be reported elsewhere.<sup>29</sup> All the peptides used in this study

- (1) Singh, R. D.; Keiderling, T. A. *Biopolymers* **1981**, *20*, 237-240.
- (2) Lal, B.; Nafie, L. A. *Biopolymers* **1982**, *21*, 2161-2183.
- (3) Sen, A. C.; Keiderling, T. A. *Biopolymers* **1984**, *23*, 1519-1532.
- (4) Sen, A. C.; Keiderling, T. A. *Biopolymers* **1984**, *23*, 1533-1545.
- (5) Narayanan, U.; Keiderling, T. A.; Bonora, G. M.; Toniolo, C. *Biopolymers* **1985**, *24*, 1257-1263.
- (6) Yasui, S. C.; Keiderling, T. A. *Biopolymers* **1986**, *25*, 5-15.
- (7) Yasui, S. C.; Keiderling, T. A.; Bonora, G. M.; Toniolo, C. *Biopolymers* **1986**, *25*, 79-89.
- (8) Narayanan, U.; Keiderling, T. A.; Bonora, G. M.; Toniolo, C. *J. Am. Chem. Soc.* **1986**, *108*, 2431-2437.
- (9) Yasui, S. C.; Sen, A. C.; Keiderling, T. A.; Toniolo, C.; Bonora, G. M. *Peptides: Structure and Function, Proceedings of the 9th American Peptide Symposium*; Deber, C. M., Hruby, V. J., Kopple, K. D., Eds.; Pierce Chemical: Rockford, IL, 1985; pp 167-172.
- (10) Lipp, E. D.; Nafie, L. A. *Biopolymers* **1985**, *24*, 799-812.
- (11) Yasui, S. C.; Keiderling, T. A. *J. Am. Chem. Soc.*, in press.
- (12) Bayley, P. M. *Prog. Biophys. Mol. Biol.* **1973**, *27*, 1-76.
- (13) Toniolo, C.; Bonora, G. M.; Bavoso, A.; Benedetti, E.; Di Blasio, B.; Pavone, V.; Pedone, C. *Biopolymers* **1983**, *22*, 205-215.
- (14) Venkataram Prasad, B. V.; Balaram, P. *CRC Crit. Rev. Biochem.* **1984**, *16*, 307-348.
- (15) Jung, G.; Brückner, H.; Schmitt, H. *Structure and Activity of Natural Peptides*; Voelter, W., Weitzel, G., Eds.; de Gruyter: Berlin, 1981; pp 75-114.
- (16) Smith, G. D.; Pletnev, V. Z.; Duax, W. L.; Balasubramanian, T. M.; Bosshard, H. E.; Czerwinski, E. W.; Kendrick, N. E.; Mathews, F. S.; Marshall, S. R. *J. Am. Chem. Soc.* **1981**, *103*, 1493-1501.
- (17) Paterson, Y.; Rumsey, S. M.; Benedetti, E.; Nemethy, G.; Scheraga, H. A. *J. Am. Chem. Soc.* **1981**, *103*, 2947-2955.
- (18) Benedetti, E.; Bavoso, A.; Di Blasio, B.; Pavone, V.; Pedone, C.; Toniolo, C.; Bonora, G. M. *Proc. Natl. Acad. Sci. U.S.A.* **1982**, *79*, 7951-7954.
- (19) Toniolo, C.; Bonora, G. M.; Benedetti, E.; Bavoso, A.; Di Blasio, B.; Pavone, V.; Pedone, C. *Biopolymers* **1983**, *22*, 1335-1356.
- (20) Wilkening, R. R.; Stevens, E. S.; Bonora, G. M.; Toniolo, C. *J. Am. Chem. Soc.* **1983**, *105*, 2560-2561.
- (21) Benedetti, E.; Bavoso, A.; Di Blasio, B.; Pavone, V.; Pedone, C.; Crisma, M.; Bonora, G. M.; and Toniolo, C. *J. Am. Chem. Soc.* **1982**, *104*, 2437-2444.
- (22) Bonora, G. M.; Mapelli, C.; Toniolo, C.; Wilkening, R. R.; Stevens, E. S. *Int. J. Biol. Macromol.* **1984**, *6*, 179-188.
- (23) Toniolo, C.; Bonora, G. M.; Barone, V.; Bavoso, A.; Benedetti, E.; Di Blasio, B.; Grimaldi, P.; Lelj, F.; Pedone, C. *Macromolecules* **1985**, *18*, 895-902.
- (24) Toniolo, C.; Bonora, G. M.; Barone, V.; Bavoso, A.; Benedetti, E.; Di Blasio, B.; Grimaldi, P.; Lelj, F.; Pavone, V.; Pedone, C. *International Forum on Peptides*, Castro, B., Martinez, J., Eds.; Hermann: Paris, in press.
- (25) Toniolo, C.; Bonora, G. M.; Benedetti, E.; Bavoso, A.; Di Blasio, B.; Pavone, V.; Pedone, C. *Int. J. Biol. Macromol.*, in press.
- (26) Toniolo, C.; Bonora, G. M.; Bavoso, A.; Benedetti, E.; Di Blasio, B.; Pavone, V.; Pedone, C. *Macromolecules* **1986**, *19*, 472-479.
- (27) Toniolo, C.; Bonora, G. M.; Bavoso, A.; Benedetti, E.; Di Blasio, B.; Pavone, V.; Pedone, C. *J. Biomol. Struct. Dyn.*, in press.

<sup>†</sup> University of Illinois at Chicago.

<sup>‡</sup> University of Padova.

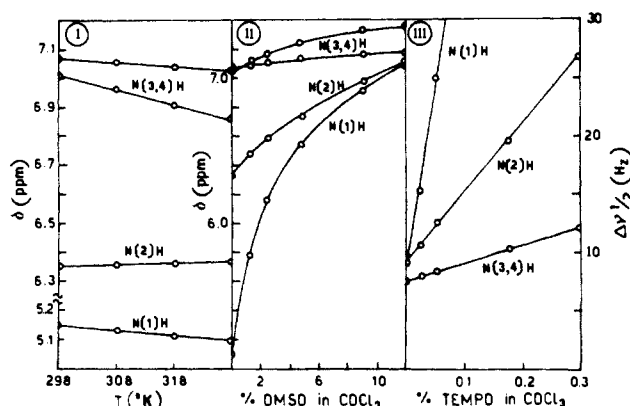


**Figure 1.** Plots of NH chemical shifts in the  $^1\text{H}$  NMR spectra of  $\text{ALA}_2$ , 4 mM in  $\text{CDCl}_3$  as a function of (I) increasing temperature, (II) increasing percentages of  $\text{Me}_2\text{SO}$  added to the  $\text{CDCl}_3$  solution (v/v), and (III) increasing percentages of TEMPO (w/v).

have been fully characterized and were found to be both chemically and optically pure.

**Methods.** The  $^1\text{H}$  NMR spectra were recorded on a Bruker WP 200 SY spectrometer. Measurements were carried out in deuteriochloroform (99.96%  $d$ ) and dimethyl- $d_6$  sulfoxide (99.96%  $d_6$ ) with tetramethylsilane as the internal standard.

VCD and IR absorption data were measured on the UIC VCD instrument.<sup>30</sup> Higher resolution IR absorption spectra were recorded with an IBM 32 FT-IR spectrometer. Spectra of  $\text{A}_n\text{LA}_2$  were obtained in  $\text{CDCl}_3$  (Aldrich) for the amide A, I, and II bands by using a variable path length cell equipped with  $\text{CaF}_2$  windows. VCD baselines were obtained with either  $Z\text{-(Aib)}_8\text{-O-}t\text{-Bu}$  ( $\text{A}_8$ ),  $Z\text{-(Aib)}_3\text{-O-}t\text{-Bu}$  ( $\text{A}_3$ ), or  $Z\text{-(Aib)}_2\text{-O-}t\text{-Bu}$  ( $\text{A}_2$ ), as appropriate, with the IR absorption intensity matched to that of the samples. From our earlier study,<sup>7</sup> it was clear that differences in aliphatic side groups between  $\text{A}_8$  and  $\text{A}_5\text{LA}_2$  had little effect on the amide IR absorption. Thus, the  $(\text{Aib})_n$  molecules provide an excellent racemic material for purposes of VCD base-line correction in this study. VCD spectra were typically collected with use of a 3-s time constant in the amide A region and a 10-s time constant in the amide I and II regions by averaging four scans with a resolution of  $\sim 12\text{ cm}^{-1}$ .

## Results

The delineation of the type of ordered conformation assumed by the  $\text{A}_n\text{LA}_2$  ( $n = 0\text{--}5$ ) peptide series in  $\text{CDCl}_3$  solution was accomplished by  $^1\text{H}$  NMR. This study includes examination of the behavior of the NH groups as a function of concentration,<sup>22,31</sup> temperature,<sup>22</sup> and addition of either the strong hydrogen-bonding acceptor solvent<sup>32</sup> dimethyl sulfoxide ( $\text{Me}_2\text{SO}$ )<sup>33</sup> or the paramagnetic free radical 2,2,6,6-tetramethylpiperidinyl-1-oxyl (TEMPO).<sup>34</sup> As an illustrative example, the results obtained for the tetrapeptide ( $n = 1$ ) are shown in Figure 1. The corresponding set of data for the octapeptide ( $n = 5$ ) has been discussed in ref 7.

In these peptides we have assigned the following unambiguously: (i) the high-field NH resonance (below 5.3 ppm) to the N-terminal residue, N(1)H, of urethane N-protected peptides;<sup>22,23,25</sup> (ii) the only doublet to the Leu NH proton; (iii) the second high-field resonance (between 6.3 and 6.4 ppm) to the N(2)H proton, by analogy with the chemical shifts of the corresponding proton in a variety of model compounds.<sup>22,23,25</sup> In the tetrapeptide ( $n = 1$ ), however, the N(2)H proton is that of the Leu residue, while in the tripeptide ( $n = 0$ ) the Leu residue is at the N-terminus of the main chain and therefore its NH proton is the urethane-type N(1)H.

**Table I.** Infrared Absorption Frequencies of  $Z\text{-(Aib)}_n\text{-L-Leu-(Aib)}_2\text{-OMe}$  ( $\text{A}_n\text{LA}_2$ ) in the Amide A, Amide I, and Amide II Regions Determined by FT-IR<sup>a</sup>

peptide	concn, M, $\text{CDCl}_3$	$\nu$ , $\text{cm}^{-1}$		
		amide A	amide I	amide II
$\text{LA}_2$	0.0207	<i>3431, 3373</i>	<i>1722, 1681</i>	1504
$\text{ALA}_2$	0.0184	<i>3430, 3359</i>	<i>1737, 1679</i>	1515, 1501
$\text{A}_2\text{LA}_2$	0.0212	<i>3426, 3346</i>	<i>1737, 1713, 1674</i>	<i>1524, 1501</i>
$\text{A}_3\text{LA}_2$	0.0187	<i>3426, 3338</i>	<i>1736, 1714, 1671</i>	<i>1530, 1501</i>
$\text{A}_4\text{LA}_2$	0.0153	<i>3427, 3329</i>	<i>1736, 1714, 1666</i>	<i>1531, 1501</i>
$\text{A}_5\text{LA}_2$	0.0147	<i>3427, 3324</i>	<i>1736, 1714, 1664</i>	<i>1532, 1500</i>

<sup>a</sup>Strong bands are italic.

A factor of 10 dilution produces a significant variation (to higher fields) of the chemical shifts of the N(1)H and N(2)H protons, which is greater for the N(1)H proton (results not shown). For the protons at lower fields, the concentration effect is negligible. The change of the temperature dependencies (i.e., slopes in Figure 1, part I) of NH chemical shifts with change in concentration (not shown) is also significant only for the N(1)H proton. The magnitude of this concentration effect decreases markedly upon decreasing peptide main-chain length.

The accessibilities of the NH protons of the  $\text{A}_n\text{LA}_2$  ( $n = 0\text{--}5$ ) peptides, indicative of a possible participation to inter- or intramolecular hydrogen bonds, were assessed as a function of temperature<sup>22</sup> and addition of  $\text{Me}_2\text{SO}$ <sup>33</sup> or TEMPO<sup>34</sup> to the  $\text{CDCl}_3$  solution. For the  $n = 1\text{--}5$  oligomers two groups of protons are observed: (i) N(1)H and N(2)H protons, whose chemical shifts are sensitive, particularly, to addition of  $\text{Me}_2\text{SO}$  and whose resonances significantly broaden upon addition of TEMPO for which the sensitivity of the N(1)H proton is significantly higher than that of the N(2)H proton (Figure 1, parts I–III); (ii) all other NH protons, whose resonances, in terms of chemical shift and linewidth, are markedly less sensitive to these environmental changes.

These  $^1\text{H}$  NMR findings, taken together, strongly support the view that, at high concentration in  $\text{CDCl}_3$  solution, the N(1)H as well as the N(2)H protons of the higher oligomers of the  $\text{A}_n\text{LA}_2$  series are involved in the intermolecular hydrogen-bonding scheme, i.e., in the self-association process, whereas all other NH protons form intramolecular hydrogen bonds. In contrast to folding, self-association can be destroyed either by heating or by addition of  $\text{Me}_2\text{SO}$  and TEMPO. Since all other NH protons (beginning from the N(3)H proton) form stable intramolecular hydrogen bonds, it may be concluded that the secondary structure adopted in  $\text{CDCl}_3$  by these peptides is the  $3_{10}$ -helix (a series of consecutive, type III  $\beta$ -turns<sup>13–16</sup>) rather than the  $\alpha$ -helix (which would have required the NH protons involved in the intramolecular hydrogen bonding to begin from the N(4)H proton). The formation to a high extent of a stable, ordered secondary structure at the tetrapeptide stage ( $n = 1$ ) in this series is additionally supported by the observation that the  $n = 1\text{--}5$  oligomers, as opposed to the  $n = 0$  oligomer (tripeptide), exhibit a magnetic nonequivalence of the benzylic  $\text{CH}_2$  protons of the benzyloxycarbonyl protecting group (Z) at the N-terminus (results not shown).

Having established the preferred conformation of the  $\text{A}_n\text{LA}_2$  oligomers in  $\text{CDCl}_3$ , we undertook the VCD and IR absorption study under comparable experimental conditions. The VCD and IR absorption spectra shown here for  $\text{A}_n\text{LA}_2$  ( $n = 0\text{--}5$ ) in  $\text{CDCl}_3$  in the amide A (Figure 2), amide I (Figure 3), and amide II (Figure 4) regions are, for purposes of clarity, divided into two plots with  $n = 0\text{--}2$  and  $n = 2\text{--}5$  superimposed separately.

In Figure 2, the IR absorption of each compound in the N–H stretching region is seen to consist of two bands. That at higher frequency ( $\sim 3427\text{ cm}^{-1}$ ) can be assigned to the free urethane and amide N–H group stretching modes and the lower, broader one ( $\sim 3330\text{ cm}^{-1}$ ) to the hydrogen-bonded N–H groups.<sup>5,7,8,17,19–23,25–27,35</sup> Table I summarizes the IR absorption frequencies of the N–H stretching bands as obtained with a

(28) Bavoso, A.; Benedetti, E.; Di Blasio, B.; Pavone, V.; Pedone, C.; Toniolo, C.; Bonora, G. M. *Proc. Natl. Acad. Sci. U.S.A.* **1986**, *83*, 1988–1992.

(29) Bavoso, A.; Benedetti, E.; Di Blasio, B.; Pavone, V.; Pedone, C.; Toniolo, C.; Formaggio, F.; Bonora, G. M., in preparation.

(30) Keiderling, T. A. *Appl. Spectrosc. Rev.* **1981**, *17*, 189–226.

(31) Iqbal, M.; Balam, P. *Biopolymers* **1982**, *21*, 1427–1433.

(32) Martin, D.; Hauthal, G. *Dimethyl Sulphoxide*; Van Nostrand-Reinhold: Wokingham, England, 1975.

(33) Pitner, T. P.; Urey, D. W. *J. Am. Chem. Soc.* **1972**, *94*, 1399–1402.

(34) Kopple, K. D.; Schamper, T. J. *J. Am. Chem. Soc.* **1972**, *94*, 3644–3646.

(35) Miyazawa, T. *Poly- $\alpha$ -Amino Acids*; Fasman, G. D., Ed.; Dekker: New York, 1967; pp 69–103.

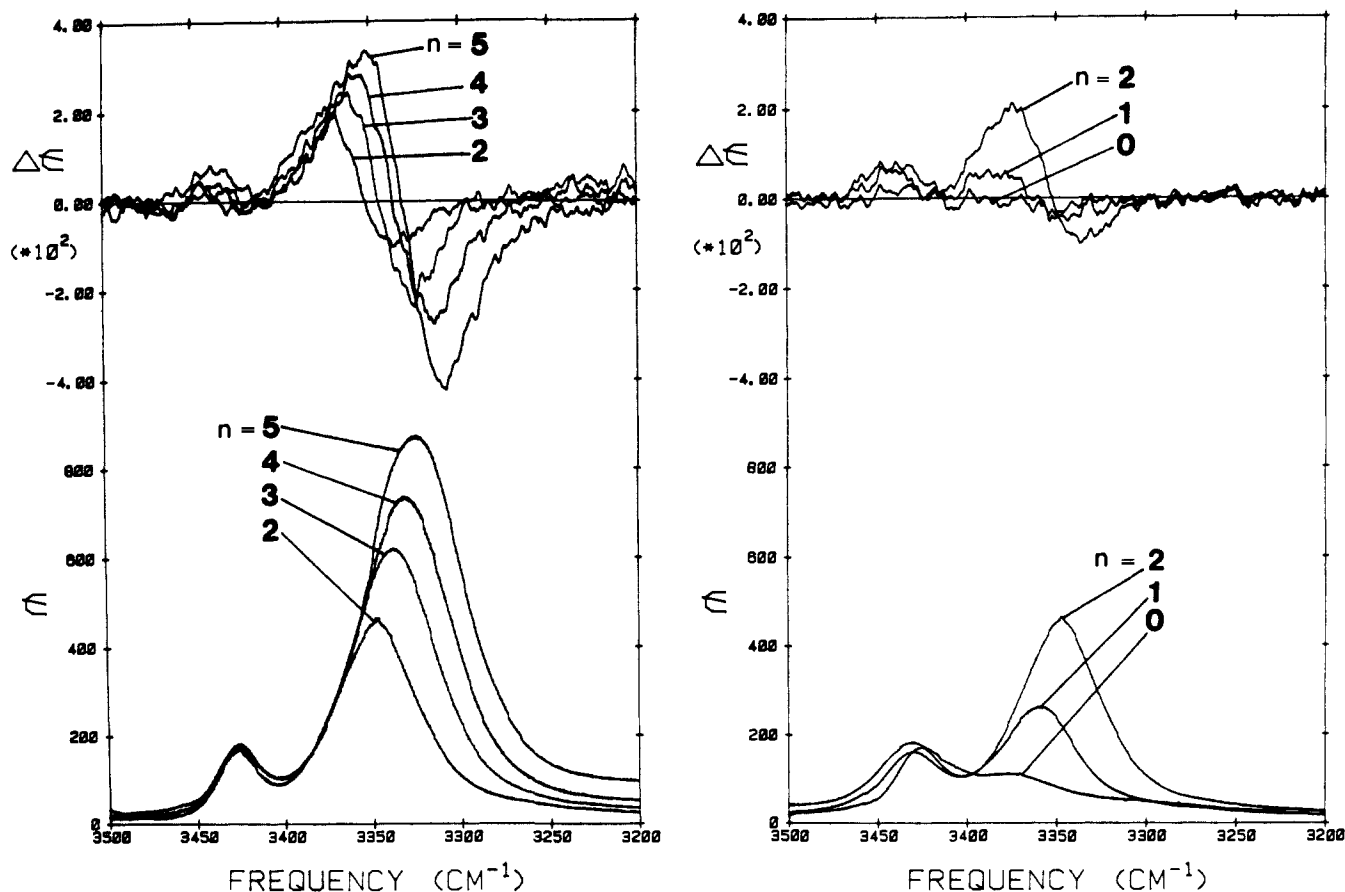


**Figure 2.** VCD and IR absorption spectra of  $A_nLA_2$  in  $CDCl_3$  solution, where  $n = 0-5$ , in the amide A region: path length 0.052 cm; four scans averaged; resolution  $\approx 12\text{ cm}^{-1}$  with 3-s time constant. Concentrations are listed in Table I, column 2.

peak-picking routine on the FT-IR spectrometer. In all but the  $n = 0$  oligomer, the hydrogen-bonded N-H band is more intense than the free N-H band and shifts to the lower frequency with increasing chain length. For  $n = 3-5$ , the VCD in the amide A region shows an almost conservative bisignate line shape with the positive lobe to higher energy. On the other hand, the VCD has a distinct positive bias for  $n = 1$  and 2 and almost no VCD for  $n = 0$ .

In the 1800–1600- $\text{cm}^{-1}$  region (Figure 3), at least three absorption bands are seen. The two bands at higher frequency can be assigned to the carbonyl stretching modes of the urethane and methyl ester protecting groups.<sup>5,7,8,17,19-23,25-27</sup> In several of the oligomers, a shoulder occurs on the low-energy side of the main amide I band (1665  $\text{cm}^{-1}$ ), both features of which are assignable to the H-bonded amide carbonyls.<sup>5,7,8,17,19-23,25-27,35</sup> The absorption band arising from the protecting C=O group in the  $n = 0$  oligomer has slightly higher intensity than the corresponding amide I band, whereas the opposite is true for  $n = 1-5$ . Additionally, the main amide I band shifts to lower frequency with increasing chain length. These FT-IR absorption frequencies are listed in Table I. The amide I band has a positive VCD couplet<sup>12</sup> (positive to lower frequency) for all except  $n = 0$ , which shows no detectable VCD. The protecting group has only a very small VCD, which is similar in sign pattern to the major VCD band arising from the amide I peak. Its bisignate nature implies a complexity beyond the above assignment. This could be due to multiple conformations accompanying intermolecular hydrogen bonding.

The main (presumably perpendicularly polarized) feature of the amide II IR absorption band (Figure 4) is centered at 1530  $\text{cm}^{-1}$  with a weaker (parallel polarization) band at 1500  $\text{cm}^{-1}$  for  $n = 2-5$  whereas for  $n = 0-1$  the lower energy component dominates. The weaker bands near 1450  $\text{cm}^{-1}$  can be assigned to hydrocarbon side-chain deformation modes. The VCD in this region has a negative monosignate band shape that correlates fairly well with the amide II IR absorption maximum for  $n = 5$  and shifts to lower energy as  $n$  decreases. The 1450- $\text{cm}^{-1}$  bands,

dominated by the asymmetric methyl deformations, yield no VCD as might be expected from the achiral Aib residues. While the  $\text{CH}_3$  and  $\text{CH}_2$  deformations of Leu also contribute to this band, their diluteness could explain their lack of VCD. Table I also summarizes the absorption band positions in the amide II region.

A summarizing plot of the magnitude of  $\Delta\epsilon/\epsilon$ , i.e.,  $|\Delta\epsilon/\epsilon|$ , as a function of  $n$  for the amide A, I, and II bands is shown in Figure 5. Here, peak-to-peak values are used to evaluate intensities of the bisignate features, and all values are plotted as being positive. In all three amide bands,  $|\Delta\epsilon/\epsilon|$  is observed to have a sharp increase for  $n = 0-2$  after which it becomes nearly constant for  $n = 3-5$ . The results for the three regions are self-consistent and imply that the  $3_{10}$ -helix is formed at  $n = 3$ .

## Discussion

Aib-rich peptide sequences are found in membrane-active, channel-forming peptaibol antibiotics that have  $3_{10}$ - and/or  $\alpha$ -helical structures.<sup>13-15,36,37</sup> In a previous paper we have demonstrated by  $^1\text{H}$  NMR, IR absorption, and VCD that  $A_3LA_2$  favors the right-handed  $3_{10}$ -helical conformation in  $CDCl_3$  solution.<sup>7</sup> As shown in Figures 2-4, the VCD data for the series  $A_nLA_2$  ( $n = 0-5$ ) have, with the exception of  $n = 0$ , qualitatively similar features as  $n$  varies. It thus appears that the whole series favors formation of a  $3_{10}$ -helix or, at least, the essential element of such a structure, i.e., a type III  $\beta$ -turn.<sup>13,14,17</sup> Furthermore, the addition of Aib residues to the N-terminus of the  $LA_2$  oligopeptide chain favors helical folding as evidenced by increased intrachain hydrogen bonding and enhanced VCD.

Intrachain H-bonding is evidenced in the IR absorption by the observed shift of the amide A and the amide I to lower frequencies and of the amide II to higher frequency and by the increase of the amide A intensity and bandwidth as the chain length increases.

(36) Nagaraj, R.; Balam, P. *Acc. Chem. Res.* **1981**, *14* 356-362.

(37) Fox, R. O., Jr.; Richards, F. M. *Nature (London)* **1982**, *300*, 325-330.

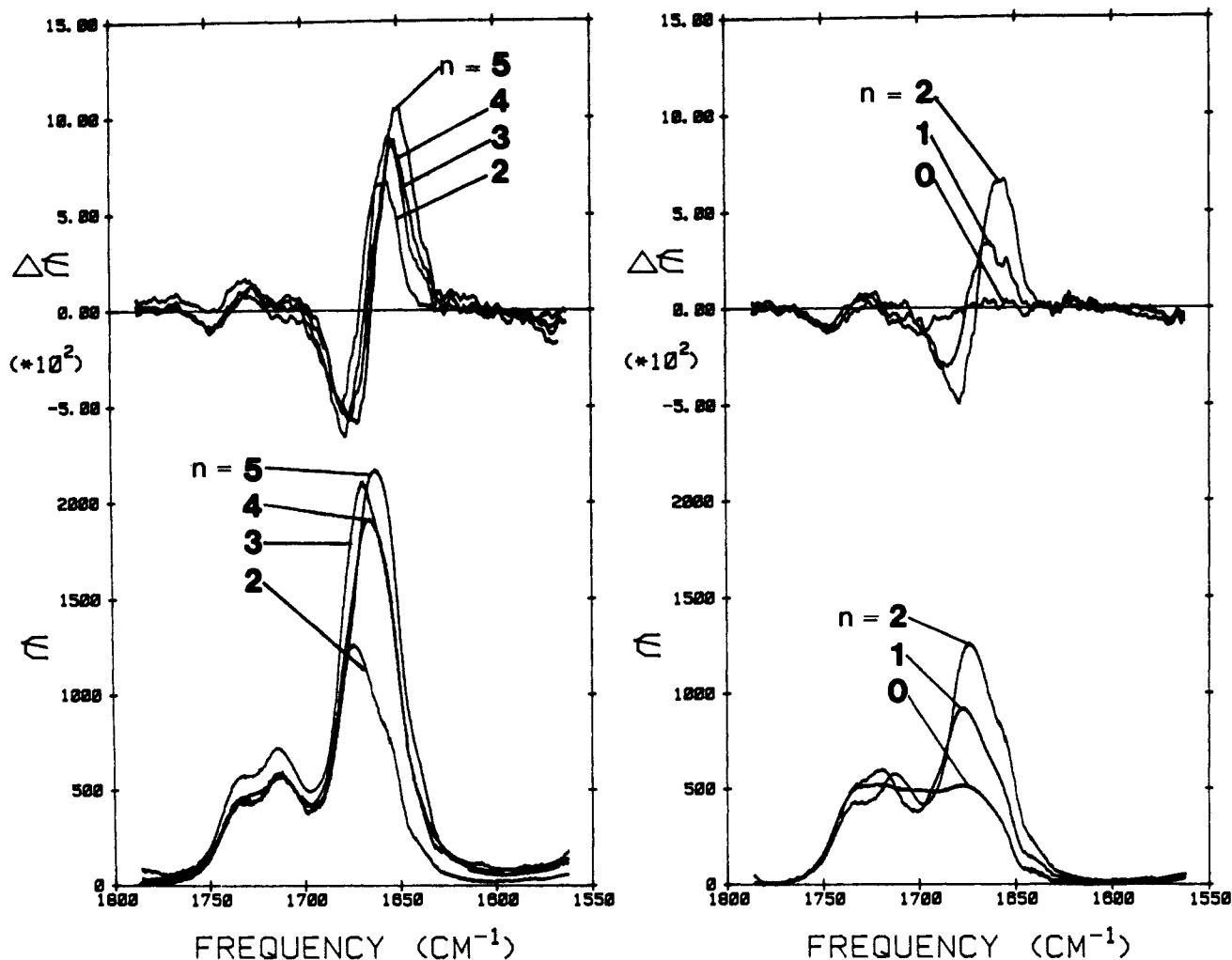


Figure 3. VCD and IR absorption spectra of  $A_nLA_2$  in  $CDCl_3$  solution, where  $n = 0-5$ , in the amide I region: path length 0.022 cm; four scans averaged; resolution  $\approx 11 \text{ cm}^{-1}$  with 10-s time constant. Concentrations are listed in Table I.

The data for NH chemical shift as a function of temperature and perturbing agents and for the magnetic nonequivalence of the benzylic  $CH_2$  protons on the N-protecting group corroborate the above conclusions. With increasing chain length, a growing number of intramolecularly hydrogen-bonded NH's are indicated in both the NMR and IR absorption spectra while the number of free or intermolecularly involved NH's is indicated to remain constant.

Comparisons of the VCD data for the  $n = 0-5$  oligomers in each of the amide regions studied also shows a steady increase of  $\Delta\epsilon$  with  $n$ . However, an important question we wish to probe is: when does the molecule attain a uniform structure? We feel that the plot of the anisotropy ratio,  $|\Delta\epsilon/\epsilon|$  vs.  $n$  (Figure 5), gives the best correlation by which one can estimate the onset of a uniform secondary structure for this series of oligopeptides. Examination of our data leads to the conclusion that a uniform secondary structure is developed by  $n = 2$  or 3. This is equivalent to almost two turns of a  $3_{10}$ -helix. Furthermore, inspection of Figures 2-4 leads to the implication that the basic structural unit of the  $3_{10}$ -helix, i.e., the type III  $\beta$ -turn, is present to a significant extent even at  $n = 1$ . This follows since the only significant changes in the VCD as  $n$  varies from 1 to 3 are ones of magnitude as opposed to band shape. At  $n = 1$ , two consecutive type III  $\beta$ -turns can be formed. This then implies that the  $3_{10}$ -helical VCD previously reported for octapeptides is an amplification of what one might find for a tetrapeptide double  $\beta$ -turn, i.e., that in a  $3_{10}$ -helix the  $\beta$ -turn contributions to VCD just add up, in phase.

It is important to realize that these conclusions are at what might be termed the "VCD level". Since the primary interaction promoting these polymeric VCD signals is assumed to be due to dipolar coupling,<sup>38-41</sup> VCD may have a shorter interaction range

for production of significant effects than does electronic CD. Thus, the structural requirements for generation of a VCD spectrum characteristic of a uniform structure may not be adequate for a parallel conclusion when analyzing electronic CD data. Since in many biopolymer situations the primary interest is in the character of a relatively local structure, this is an advantage for VCD studies. In particular, this aspect of VCD should enable its detailed application to conformational study of globular proteins where sections of uniform secondary structure are, by definition, limited in length.<sup>9</sup>

It is worth noting that  $\alpha$ -helices and  $3_{10}$ -helices have been observed to be indistinguishable by electronic CD and IR absorption.<sup>42</sup> On the basis of our data, it appears that VCD can distinguish the two structures by using both band shape and relative magnitude arguments. The  $\alpha$ -helical amide A is strongly positively biased while that of the  $3_{10}$ -helix is nearly symmetrical. The  $\alpha$ -helical amide I is negatively biased and intense while that of  $3_{10}$ -helix is only slightly positively biased and is weak. The  $\alpha$ -helical amide II VCD is significantly lower in energy than the absorbance maximum while in the  $3_{10}$ -helix they are close in frequency. This problem of distinguishing two similar structures

(38) Schellman, J. A. In *Peptides, Polypeptides and Proteins*; Blout, E. R., Bovey, F. A., Goodman, M., Lotan, N., Eds.; Wiley: New York, 1974; pp 320-337.

(39) Snir, J.; Frankel, R. A.; Schellman, J. A. *Biopolymers* 1975, 14, 173-196.

(40) Deutsche, C. W.; Moscovitz, A. *J. Chem. Phys.* 1968, 49 3257-3272.

(41) Deutsche, C. W.; Moscovitz, A. *J. Chem. Phys.* 1970, 53, 2630-2644.

(42) Sudha, T. S.; Vijayakumar, E. K. S.; Balaram, P. *Int. J. Pept. Protein Res.* 1983, 22, 464-468.

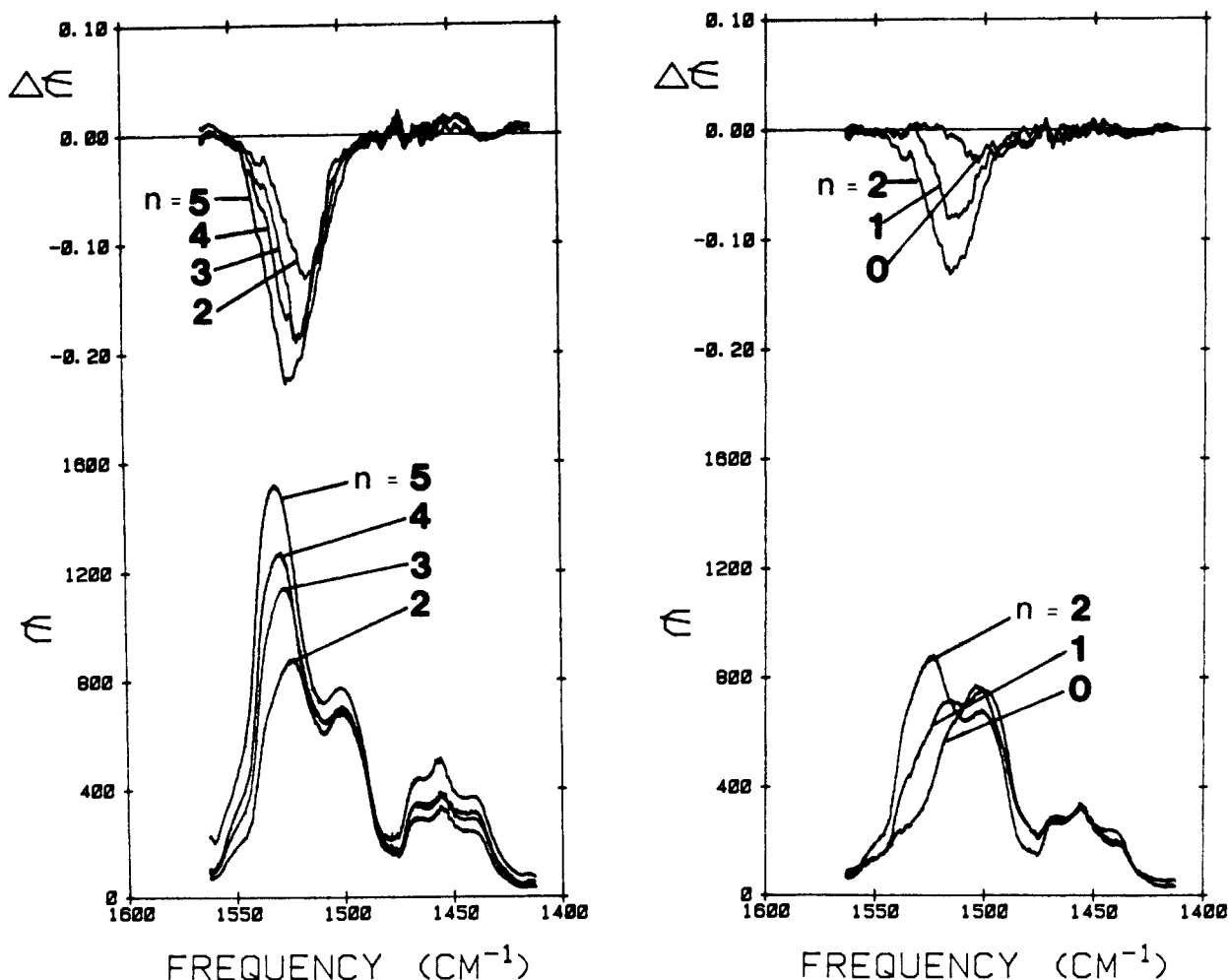


Figure 4. VCD and IR absorption spectra of  $A_nLA_2$  in  $CDCl_3$  solution, where  $n = 0-5$ , in the amide II region: path length 0.042 cm, as in Figure 3.

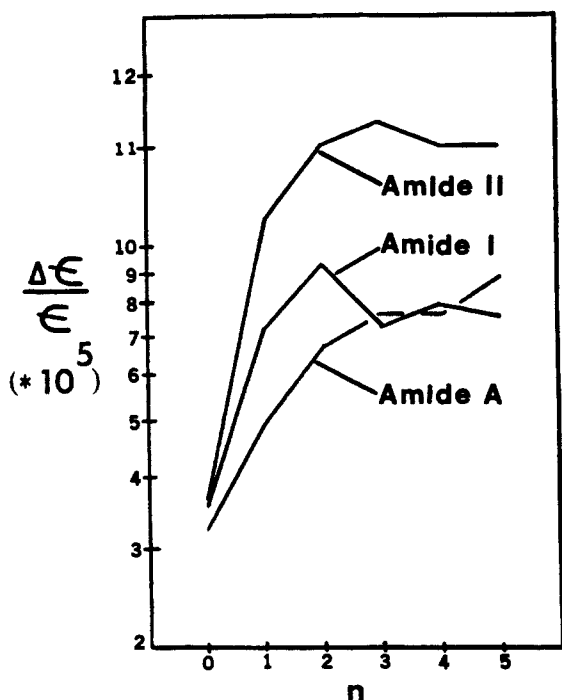


Figure 5. Comparison of  $|\Delta\epsilon/\epsilon|$  values as a function of  $n$  for  $A_nLA_2$  where  $n = 0-5$ , for the amide A, I, and II bands ( $\approx 3330$ ,  $1665$ , and  $1530\text{ cm}^{-1}$ , respectively).

provides a very nice example of the power of VCD, as compared to other chiroptical techniques, to study several independent,

nonoverlapped bands and to use the total information derived to establish a more detailed interpretation of the molecular conformation.

In such an analysis of  $3_{10}$ -vs.  $\alpha$ -helices, it must be made clear that comparable short-chain  $\alpha$ -helices are not available to us.<sup>7</sup> While our data imply that the  $3_{10}$ -helix has a stable  $\Delta\epsilon/\epsilon$  value when it achieves the hexamer ( $n = 3$ ) level, we cannot *absolutely* rule out that a second change in  $\Delta\epsilon/\epsilon$  might occur at a substantially longer chain length<sup>5,8</sup> or that short  $\alpha$ -helices could give different VCD than that published for polypeptides.<sup>2,3,6</sup> However, with respect to our above discussion of short- vs. long-range interactions, it must be reiterated that we expect further length-dependent changes in the spectra to be unlikely at the VCD level.

Finally, some comment is in order with regard to the value of VCD as opposed to IR absorption alone for biopolymer structural analysis. It is clear from Figure 2 that, by using just the frequency shift or the  $\epsilon$  value of the amide A per peptide unit, one would come to a different conclusion as regards formation of a uniform secondary structure. The peak frequency for the amide A continues to shift to lower energy for  $n = 0-5$ , while  $\epsilon$  per peptide unit stabilizes. In the amides I and II regions, parallel analyses of the IR absorptions do not obtain. However, from Figure 5, we can see that the VCD analyses of all three bands is self-consistent in terms of  $|\Delta\epsilon/\epsilon|$ . This property leads us to conclude that the combination of VCD with IR absorption is a significantly stronger stereochemical tool than is IR absorption alone.

Furthermore, it is clear by extension that combining VCD, IR absorption, NMR, and electronic CD will yield more detailed and precise analyses of biopolymer conformation than any one of these methods alone. Having all these techniques at the peptide chemist's disposal is important because in many cases one or the other cannot be used. For example, electronic CD studies of

peptides in  $\text{CHCl}_3$  solvents cannot be done successfully due to solvent interference in the far-UV. Our goal in this work is to develop the basis set of conformationally characteristic peptide spectra for the newest technique, VCD, to a level where it will truly develop into a practical tool.

**Acknowledgment.** We thank the National Institutes of Health

(Grant GM-30147, T.A.K.) for partial support of this research and the Research Board of the University of Illinois for partial purchase of the FT-IR spectrometer.

Registry No. LA<sub>2</sub>, 103003-66-3; ALA<sub>2</sub>, 103003-67-4; A<sub>2</sub>LA<sub>2</sub>, 103003-68-5; A<sub>3</sub>LA<sub>2</sub>, 103003-69-6; A<sub>4</sub>LA<sub>2</sub>, 103003-70-9; A<sub>5</sub>LA<sub>2</sub>, 100817-47-8.

## On the Addition of Silyl Radicals to Unsaturated Carbonyl Compounds: Regioselectivity of the Attack and 1,3 Carbon to Oxygen Silicon Migration

Angelo Alberti,\*<sup>†</sup> Chryssostomos Chatgililoglu,<sup>†</sup> Gian Franco Pedulli,\*<sup>†</sup> and Paolo Zanirato<sup>§</sup>

Contribution from the Istituto dei Composti del Carbonio Contenenti Eteroatomi e loro Applicazioni, CNR, 40064 Ozzano Emilia, Italy, Istituto di Chimica Organica dell'Universita', 40136 Bologna, Italy, and Istituto di Chimica Organica dell'Universita', 09100 Cagliari, Italy. Received January 22, 1986

**Abstract:** The addition reactions of silyl radicals with 2,6-di-*tert*-butyl- (1), 2,6-dimethoxy- (2), and 2,6-dimethyl-*p*-benzoquinone (3), 3,6-dimethylthieno[3,2-*b*]thiophene-2,5-dione (4), 9-methyleneanthrone (5), and 5-benzylidene-3,6-dimethylthieno[3,2-*b*]thiophen-2-one (6) have been studied by EPR spectroscopy. With substrates 5 and 6 only the adducts resulting from attack at the exocyclic olefinic double bond were detected up to 400 K. With the quinones and dithiolactone 4 the nature of the adducts depended on the experimental temperature: thus at low temperature preferential addition of silyls to the less hindered ring carbon atom was evident, while at higher temperature only the adducts to a carbonyl oxygen were detected. Experimental evidence has been obtained that the kinetically favored carbon adduct converts to the thermodynamically more stable oxygen adduct via a 1,3 carbon to oxygen internal migration of the organometallic group involving a four-membered cyclic transition state. The kinetics of the rearrangement has been followed for the triphenylsilyl adduct of 1 and the Arrhenius equation  $\log(k/s^{-1}) = [(13.8 \pm 0.3) - (18.2 \pm 0.3)]/\theta$  was determined. The rearrangement of the corresponding adduct of 4 was much slower and its kinetic analysis was complicated by a fast equilibration with its dimer. A kinetic scheme is outlined according to which the observed rate constants should refer to the rearrangement of the dimer rather than of the radical. An alike behavior is also reported for the triphenylgermyl adducts of compounds 1 and 4.

It is well established that for molecules undergoing radical addition and containing both olefinic and carbonylic double bonds the preferred site of attack by carbon-centered radicals is the weaker C=C ( $\pi\text{BDE}^1$  ca. 60 kcal/mol) rather than the C=O bond which is some 15 kcal/mol stronger.<sup>2</sup> Silyl radicals, in view of the exothermicity of their reactions with unsaturated derivatives, should attack preferentially C=C double bonds. Actually, in recent kinetic investigations, Ingold and co-workers showed that the rates of addition of trialkylsilyl radicals to olefins (ca.  $10^6$  to  $10^7 \text{ M}^{-1} \text{ s}^{-1}$ )<sup>3</sup> were about an order of magnitude higher than those for the addition to structurally related ketones (ca.  $10^5$  to  $10^6 \text{ M}^{-1} \text{ s}^{-1}$ ).<sup>4</sup>

Indeed, the low-temperature reaction of silyl radicals with isopropenyl acetate<sup>5</sup> or maleic anhydride<sup>6</sup> led to the EPR detection of species resulting from the addition to the olefinic double bonds;

yet, in the large majority of reactions between silyls and unsaturated carbonyl compounds, only addition to C=O double bonds was observed.<sup>7</sup> Although the preferential formation of oxygen adducts was justified<sup>7a</sup> on thermodynamic basis with the greater strength of the O-Si bond thus formed (119–128 kcal/mol)<sup>8,9</sup> if compared with that of the C-Si bond (89 kcal/mol),<sup>9</sup> it remains in contradiction with expectation. This behavior can, however, be accounted for by two alternative reaction pathways involving as a first step the kinetically favored addition of  $\text{R}_3\text{Si}^\cdot$  to the C=C double bond. Subsequently, the so formed primary radicals may evolve to the thermodynamically more stable oxygen adducts either by cleavage of the C-Si bond followed by readdition to the carbonyl group or by an intramolecular carbon to oxygen migration of silicon through a cyclic transition state. The former mechanism implies reversibility of the addition of silyls to unsaturated carbons which is known to be unimportant for the adducts to simple olefins.<sup>10</sup> The latter mechanism seems more reasonable in view

<sup>†</sup> Istituto CNR, Ozzano Emilia.

<sup>†</sup> Universita' di Cagliari.

<sup>§</sup> Universita' di Bologna.

(1) (a) Citterio, A.; Minisci, F.; Vismara, E. *J. Org. Chem.* **1982**, *47*, 81–88. (b) Giese, B.; Kretzschmar, G. *Chem. Ber.* **1982**, *115*, 2012–2014 and references cited.

(2) Golden, D. M.; Benson, S. W. *Chem. Rev.* **1969**, *69*, 125.

(3) Chatgililoglu, C.; Ingold, K. U.; Scaiano, J. C. *J. Am. Chem. Soc.* **1983**, *105*, 3292–3296.

(4) Chatgililoglu, C.; Ingold, K. U.; Scaiano, J. C. *J. Am. Chem. Soc.* **1982**, *104*, 5119–5123.

(5) Bowles, A. J.; Hudson, A.; Jackson, R. A. *J. Chem. Soc. B* **1971**, 1947–1949.

(6) Alberti, A.; Hudson, A.; Pedulli, G. F. *Tetrahedron* **1982**, *38*, 3749–3752.

(7) (a) Cooper, J.; Hudson, A.; Jackson, R. A. *J. Chem. Soc., Perkin Trans. 2* **1973**, 1933–1937. (b) Alberti, A.; Hudson, A. *J. Chem. Soc., Perkin Trans. 2* **1978**, 1098–1102. (c) Chen, K. S.; Foster, T.; Wan, J. K. S. *Ibid.* **1979**, 1288–1292. (d) Adeleke, B. B.; Wan, J. K. S., *Ibid.* **1980**, 225–228. (e) Alberti, A.; Hudson, A.; Pedulli, G. F.; Zanirato, P. *J. Organomet. Chem.* **1980**, *198*, 145–154.

(8) Jackson, R. A. *Spec. Publ.—Chem. Soc.* **1970**, No. 24, 295–321.

(9) Walsh, R. *Acc. Chem. Res.* **1981**, *14*, 246–252.

(10) (a) Bennett, S. W.; Eaborn, C.; Jackson, R. A.; Pearce, R. *J. Organomet. Chem.* **1968**, *15*, P17–P17. (b) Jackson, R. A. *J. Chem. Soc., Chem. Commun.* **1974**, 573–574. (c) Chatgililoglu, C.; Woynar, H.; Ingold, K. U.; Davies, A. G. *J. Chem. Soc., Perkin Trans. 2* **1983**, 555–561.